

FACILITY FORM 62

N 66-17 260  
 (ACCESSION NUMBER)  
 27  
 (ISSUE)  
 30  
 (CODE)  
 (CATEGORY)

X-643-65-420

55388

# NUMERICAL DETERMINATION OF SHORT PERIOD TROJAN ORBITS IN THE RESTRICTED THREE BODY PROBLEM

BY  
**EDSON F. GOODRICH**

GPO PRICE \$ \_\_\_\_\_

CFSTI PRICE(S) \$ \_\_\_\_\_

Hard copy (HC) 2.00

**OCTOBER 1965**

Microfiche (MF) 1.50

ff 653 July 65

**NASA**

**GODDARD SPACE FLIGHT CENTER**

**GREENBELT, MARYLAND**

X-643-65-420

**NUMERICAL DETERMINATION OF SHORT PERIOD TROJAN ORBITS  
IN THE RESTRICTED THREE BODY PROBLEM**

by

**Edson F. Goodrich**

**Goddard Space Flight Center  
Greenbelt, Maryland**

# Numerical Determination of Short Period Trojan Orbits in the Restricted Three Body Problem

Edson F. Goodrich

## ABSTRACT

In the plane restricted three body problem, two classes of periodic orbits exist around the equilateral libration points. Rabe developed methods for determining members of the class of long period orbits with Jupiter and the Sun as principal masses. This report demonstrates the use of these methods to examine the class of short period orbits. Power series expansions permit the solution of the relevant equations of motion on an IBM 7094 computer; closed form recurrence formulae allow the computation of the coefficients of the power series. Knowledge of the value for the Jacobi constant gives approximate initial conditions for short period orbits near the libration points. An iteration scheme improves the initial conditions to periodic conditions. For the starting positions used, two types of short period orbits are computed with an accuracy of twelve significant figures. The Jacobi constant decreases as the orbit size increases and deviates farther from the libration point. The periods of all orbits differ by less than one percent from the period of Jupiter's motion around the Sun. Elliptical orbits around the Sun closely represent the short period orbits, and the eccentricities of these elliptical orbits approach unity as the deviations from the libration point increase. A linear stability study indicates instability for all orbits determined.

## 1. INTRODUCTION

The restricted problem of three bodies involves the study of the motion of an infinitesimal particle moving under the influence of two finite point masses and is one of the classical problems in celestial mechanics. Studies show the existence of periodic orbits of the infinitesimal mass about the two equilateral Lagrangian libration points. These periodic orbits fall into two general classifications consisting of short period and long period orbits. The short period orbits have periods on the order of the period of the two principal masses about their common center of mass. The periods of long period orbits depend on the mass ratio of the finite masses. With the Sun and Jupiter as predominant masses, these orbital periods are on the order of twelve times the period of Jupiter's motion around the Sun.

Most numerical investigations give results of a few significant figures. Rabe (1961) showed to a high degree of accuracy that orbits exist for the class of long period orbits. To a limited degree of accuracy, Willard (1913) examined the short period orbits. This present work is an effort to characterize, to a high degree of accuracy, the family of short period orbits.

Steffensen (1956) developed a numerical integration scheme for solving the equations of motion in which he introduced two auxiliary variables and expanded the coordinates in powers of the time. He derived recurrence formulae in closed form for the coefficients of the power series.

For the case considered, the Sun and Jupiter represent the predominant masses and a Trojan asteroid represents the infinitesimal mass. By assumption, the Sun and Jupiter move about their common center of mass in concentric circles

undisturbed by the Trojan's presence and the Trojan remains in the plane of the orbits of the Sun and Jupiter.

The x-y reference system used has its origin at Jupiter and rotates with uniform angular velocity with the Sun fixed in the system on the positive x-axis. The unit of distance is the Jupiter-Sun distance, the unit of mass is the mass of the Sun, and the unit of time is such that the gravitational constant is unity. If  $M$ ,  $N$ , and  $P$  represent the mass, mean motion, and period of Jupiter respectively, then  $N^2 = 1 + M$  and  $P = 2\pi/N$ . For this study,  $M = .00095478610$  from Hill's value for the mass ratio of Jupiter and the Sun.

Modification of one of the auxiliary variables of Steffensen's method by the factor  $M$ , as suggested by Rabe (1961), speeds convergence of the power series. Steffensen's method is ideally suited for use with a high speed computer. Approximate starting conditions for a periodic orbit of short period used with an iterative procedure yield periodic orbits of high precision. This report considers orbits around libration point  $L_5$ . Symmetry considerations yield results for orbits around the other equilateral libration point  $L_4$ .

## 2. DETERMINATION OF APPROXIMATE INITIAL CONDITIONS

Finding periodic orbits by an iteration procedure requires starting values  $x_0, y_0, \dot{x}_0, \dot{y}_0$  which result in a return of the particle to the near vicinity of the starting position with velocity components of the same order of magnitude and algebraic sign as the initial values. To find the initial conditions for the long period orbits, Rabe assumed that, at a point A, the first and second derivatives of the velocity with respect to time were zero. This starting point on the line joining the Sun and  $L_5$  is such that  $L_5$  lies between the Sun and the point A as shown in Fig. 1. This assumption enables the derivation of a quadratic

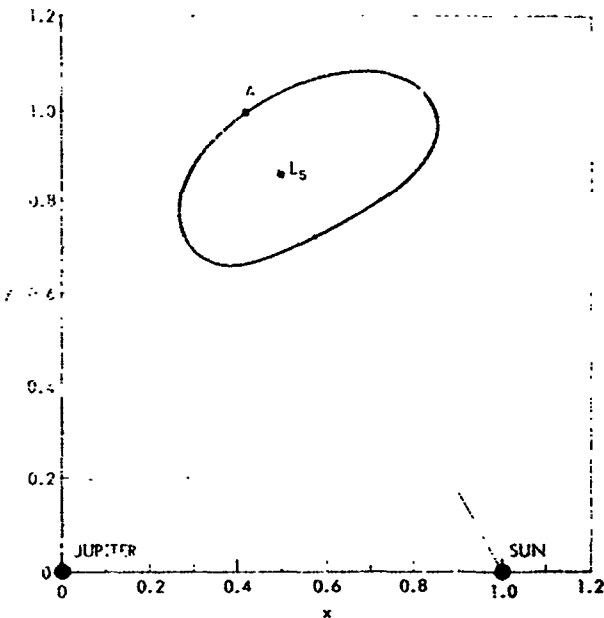


Figure 1—The rotating coordinate system with a typical periodic orbit.

expression for the initial velocity components in terms of position. The smaller of the two roots to this equation proves satisfactory for the approximate long period orbit starting conditions. The larger root to the quadratic should yield a good approximation for starting the short period orbits, but trial results proved negative. The large first and second derivatives for those orbits invalidate the quadratic expression.

For long period orbits, the velocity at point A is nearly perpendicular to the line SA connecting the Sun and the point A. This should hold for short period orbits which deviate only slightly from the libration point. The final results verify this. If  $\rho$  represents the ratio of velocity components at the starting point such that  $\rho = \dot{y}_0 / \dot{x}_0$  at  $t = 0$ , then  $\rho$  is approximately .577 for small orbits. Furthermore, for short period orbits, Charlier (1905), shows that the Jacobi integral yields  $C < 3(1 + M)$  where  $C$  is the Jacobi constant. This inequality relates the initial position to the initial velocity,  $v = (\dot{x}_0^2 + \dot{y}_0^2)^{1/2}$ . These two conditions permit the determination of good approximate initial velocity components for starting positions along the line SA and near to the libration point.

### 3. ITERATION TO A PERIODIC ORBIT

An IBM 7094 digital computer performs the computations involved in double precision. The approximate starting position components  $x_0$ ,  $y_0$  and velocity components  $\dot{x}_0$ ,  $\dot{y}_0$  are read into the computer along with the time interval and tolerance desired for the numerical integration. The step-by-step integration terminates when the trajectory approaches the starting point A and crosses the line SA. The point of crossing is found to a high degree of accuracy, the final time interval adjusts such that, within the tolerance specified, the final point of the orbit coincides with a point on SA. The orbit does not close since the initial conditions approximated periodic conditions. We must now improve the orbit.

Holding the starting position fixed, we must alter the initial velocity such that the orbit is periodic. If the subscript f denotes the final values of the components, then  $y_f = y(x_f)$  since the end position is forced to lie on SA. From the Jacobi integral,  $C = C(x_f, y_f, \dot{x}_f, \dot{y}_f)$ , and for points along SA greater than one unit from the Sun, C is monotone increasing. Therefore, if  $\dot{x}_f$  and  $\dot{y}_f$  are equal to  $\dot{x}_0$  and  $\dot{y}_0$  respectively,  $x_f = x_0$  and  $y_f = y_0$  since C remains constant. A differential correction procedure proves satisfactory for improving the initial conditions for orbits with small values of  $\lambda$ , where  $\lambda$  is the distance from A to the libration point. This method fails for values of  $\lambda$  greater than approximately .50.

A brute force method used in this difficult region actually works for any value for  $\lambda$ . With this method, the velocity components for a given  $\lambda$  are specified in terms of  $\rho$  and  $\nu$ . A small arbitrary change made in  $\rho$  while holding  $\nu$  fixed permits the computation of the change in the quantity  $\Delta\dot{x} = \dot{x}_f - \dot{x}_0$  with respect

to  $\rho$ . Linear interpolation gives a new value for  $\rho$  which forces  $\Delta\dot{x}$  toward zero.  $\Delta\dot{x}$  decreases by several orders of magnitude rather than become zero since the system is nonlinear. Repetition of the procedure reduces  $\Delta\dot{x}$  to the required tolerance. Now introduce a small arbitrary change in  $\nu$ . This causes  $\Delta\dot{x}$  to become large again and  $\rho$  must again be adjusted until  $\Delta\dot{x}$  meets the tolerance. These two sets of starting conditions with  $\Delta\dot{x}$  arbitrarily small permit the computation of a new value for  $\nu$  which forces  $\Delta\dot{y} = \dot{y}_f - \dot{y}_0$  toward zero. Again, the reduction is by several orders of magnitude. Iteration of this process forces  $\Delta\dot{x}$  and  $\Delta\dot{y}$  to meet the tolerance. This procedure works best if the arbitrary changes in  $\rho$  and  $\nu$  cause  $\Delta\dot{x}$  and  $\Delta\dot{y}$  to change sign and decrease in absolute value.

Computing the Jacobi constant and noting any resulting change provides a continuous check on the computational accuracy. Variations in  $C$  indicate corresponding errors in the accuracy of the results. The converse is not true, however, since  $C$  can remain constant though errors exist in the results. Solving the equations of motion using a high order Runge-Kutta integration scheme provides a final check on the results. Examination of the final periodic orbits in this manner shows all orbits correct to at least twelve significant figures.

#### 4. FINDINGS ON THE SHORT PERIOD ORBITS

Periodic orbits were found for values of  $\lambda$  beginning with  $\lambda = .02$  and increasing in equal intervals of  $.02$  up to  $\lambda = .50$ . When plotted in the rotating frame of reference, the first orbits determined appear to be elliptical in shape as shown in Fig. 2. The shape changes as  $\lambda$  increases beyond a value of about  $.24$  where the side nearest the Sun flattens out and eventually bends inward toward  $L_2$  and away from the Sun. As  $\lambda$  increases further, the orbits dip closer



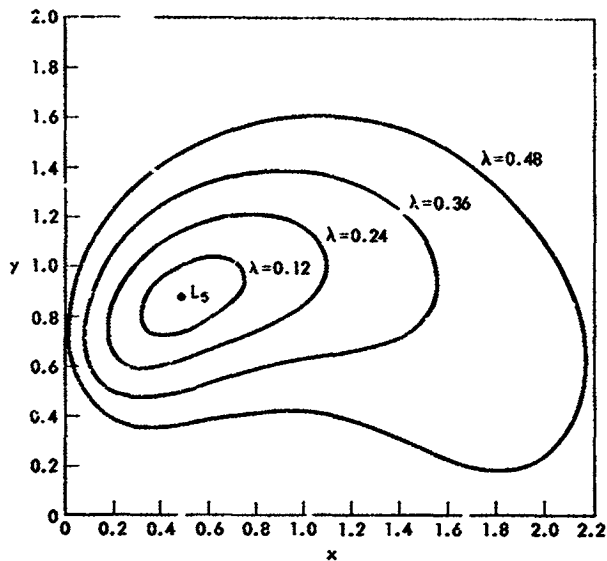


Figure 2—Short period orbits for  $\lambda = .12, .24, .36, .48$ .

and closer to the x-axis in the vicinity of the libration point  $L_3$  as illustrated in Fig. 2. Finally, as seen in Fig. 3, the orbits cross the x-axis.

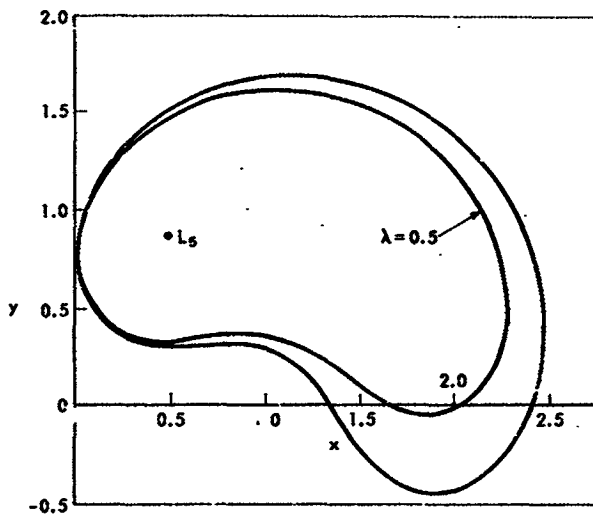


Figure 3—Short period orbit for  $\lambda = .50$  and the branch point orbit.

An attempt to iterate initial conditions for  $\lambda = .52$  to a periodic orbit failed. Further examination revealed that two different periodic orbits exist for  $\lambda = .514$ , no periodic orbit of this type exists for  $\lambda = .515$  and indeed two orbits exist for value of  $\lambda$  below some branch point value where the orbits are identically the same orbit. This branch point orbit, shown in Fig. 3, occurs at  $\lambda = .514\ 325\ 370$ .

As  $\lambda$  decreases from the branch point, the second type of orbit dips further below the x-axis and passes closer and closer to the Sun. Passing near the Sun results in large coefficients of the power series expansions; and for passage too close, the coefficients exceed the computer's capacity. A reduction of the time interval decreases the number of terms required in the expansion; however, the powers of the time interval become too small for the machine. As a result, we show the second type of orbit for values of  $\lambda$  only down to  $\lambda = .36$ . Figure 4 represents several of these orbits.

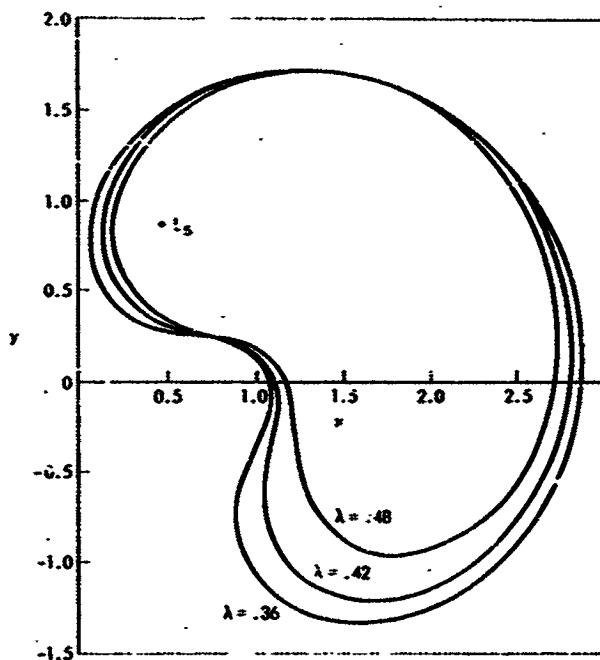


Figure 4—Type II short period orbits for  $\lambda = .48, .42, .36$ .

Call the smaller of the two orbits for a given  $\lambda$  Type I, and call the larger Type II. Figure 5 identifies the two orbits for  $\lambda = .40$ . All Type II orbits cross the x-axis. Type I orbits for  $\lambda = .48$  and less do not cross the x-axis, but for  $\lambda = .50$  and greater they do cross. For  $\lambda = .496\ 690\ 858$ , the orbit just touches the x-axis in the neighborhood of  $x = 1.85$ .

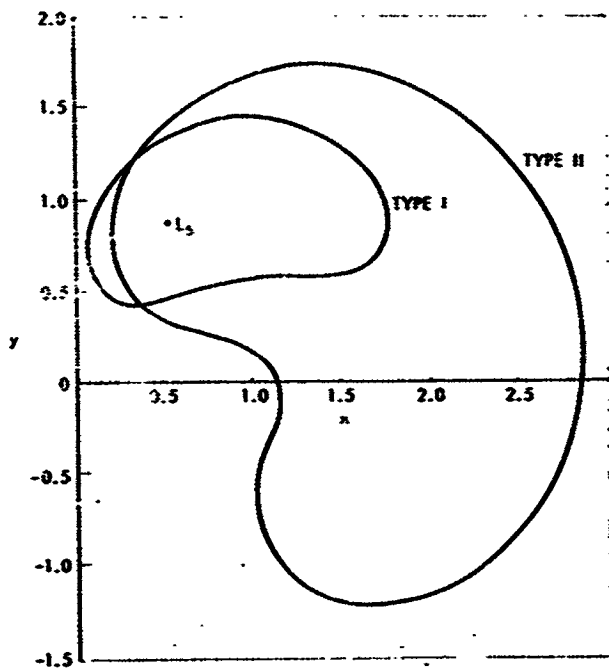


Figure 5—Type I and Type II short period orbits for  $\lambda = .40$ .

## 5. STARTING CONDITIONS AND ORBIT PERIODS

Table I and Table III give initial position and velocity components for Type I and Type II orbits respectively. The  $x_0$  and  $y_0$  coordinates depend linearly on  $\lambda$ . Both components of velocity increase for Type I orbits as  $\lambda$  increases to the branch point. For Type II orbits, as  $\lambda$  decreases from the branch point,  $\dot{x}_0$  decreases but  $\dot{y}$  increases. The branch point values for quantities in these tables are  $x_0 = .242\ 837\ 315$ ,  $y_0 = 1.311\ 444\ 240$ ,  $\dot{x}_0 = .749\ 352\ 314$ ,  $\dot{y}_0 = .829\ 243\ 523$ .

Tables II and IV list the values for the period  $T$  and the Jacobi constant  $C$  as well as  $\rho$  and  $\nu$  for Type I and Type II orbits respectively. Branch point values are  $\rho = 1.106\ 613\ 681$ ,  $\nu = 1.117\ 664\ 400$ ,  $T = 6.284\ 760\ 760$ ,  $C = 2.367\ 857\ 918$ . Figure 6 shows a plot of  $\rho$  vs  $\lambda$  for short period orbits.  $\rho$  increases nearly linearly with  $\lambda$  for Type I orbits until  $\lambda = .40$ . Figure 7 is a

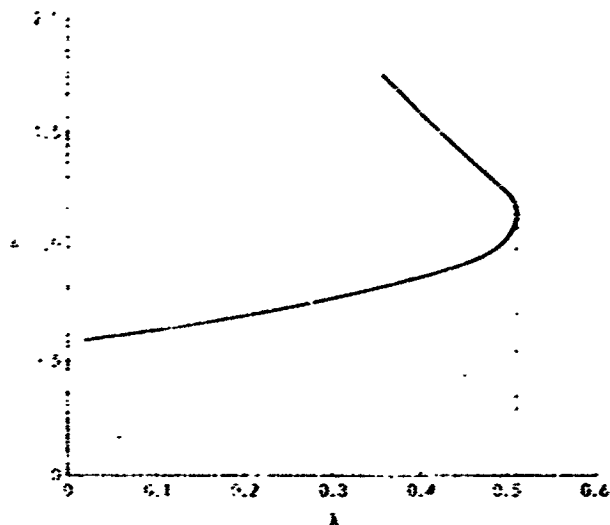


Figure 6—Variation of  $\nu$  with  $\lambda$  for periodic orbits.

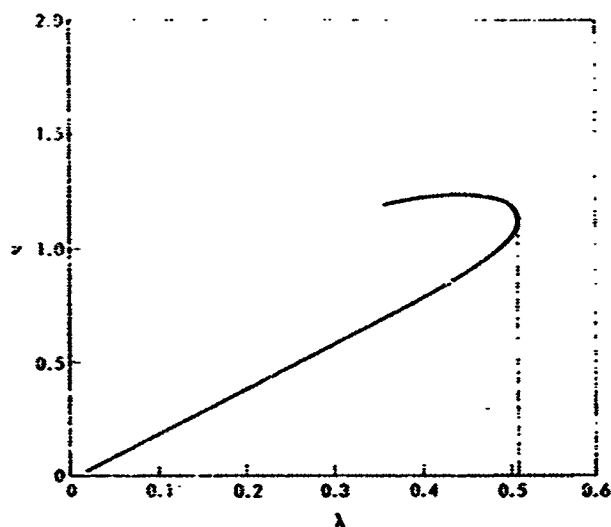


Figure 7—Variation of  $\nu$  with  $\lambda$  for periodic orbits.

similar plot of  $\nu$  vs  $\lambda$ . Again the behavior is nearly linear until  $\lambda = .40$ .  $\nu$  reaches a maximum (at least a local maximum) of just over 1.20 in the neighborhood of  $\lambda = .44$  for the Type II orbits.

The period and Jacobi constant decrease with increasing  $\lambda$  for Type I orbits. They continue to decrease as  $\lambda$  decreases from the point for Type II orbits. Notice that in the vicinity of  $\lambda = .42$  there exists an orbit for which the period equals the period of Jupiter,  $P = 6.280\ 187\ 905$ .

In a nonrotating frame of reference these short period Trojans move in perturbed elliptical two-body orbits with the Sun as the principal body and with Jupiter supplying the disturbing force in a periodic manner. An ellipse will, therefore, approximate the Trojan motion. Using the initial position and velocity in the fixed reference system, we compute the semi-major axis,  $a$ , and the eccentricity,  $e$ , as the approximating elliptical elements for each orbit. Table V and Table VI list  $a$  and  $e$  for Type I and Type II orbits respectively. For the branch point orbit,  $a = 1.001\ 076\ 088$  and  $e = .730\ 135\ 639$ .

## 6. COMPARISON WITH LONG PERIOD ORBITS

Notice the slight variations of the periods over the entire range of orbits computed. The period deviates less than one-third of one percent from the period of Jupiter. Contrast this with the long period orbits which range from about six times the orbital period of Jupiter to an orbit of infinite period.

For Type I short period orbits, the value of the Jacobi constant approaches the quantity  $3(1+M)$  from below as  $\lambda$  approaches zero. For the long period orbits,  $C$  tends toward the same value from above as  $\lambda$  goes to zero. A plot of the long period orbit with the short period orbit for  $\lambda = .02$  in Fig. 8 shows the relative sizes of the two orbits.

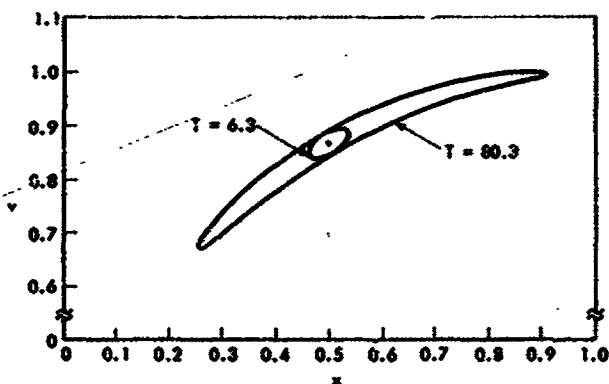


Figure 8—Short and long period orbits for  $\lambda = .02$ .

As  $\mu$  increases, the long period orbits take on a horseshoe shape and are quite different from the short period orbits which only gradually bend around the Sun. It appears that, as  $\mu$  decreases the Type II orbits will take on the horseshoe shape, though they will be much thicker than the long period orbits and not symmetrical with respect to the x-axis.

For the short period orbits, the initial velocities exceed those for the corresponding long period orbits. This accounts for the shorter periods and lower values of the Jacobi constant for the short period orbits.

## 7. LINEAR STABILITY

To examine the stability of the short period orbits, we use Hill's first order equation

$$\frac{d^2\eta}{du^2} + \Theta(u)\eta = 0,$$

as treated by Message (1959) and Rabe (1961). In this equation,  $\eta$  represents the transversal displacement of a Trojan deviating from a periodic reference orbit in some disturbed trajectory. If  $m = \frac{2\pi}{T}$ , then  $u = m(t-t_0)$  defines the new independent variable. Knowing a set of special values for points along the orbit, we expand the function  $\Theta(u)$  in a Fourier series of the form

$$\Theta(u) = \left(\frac{N}{m}\right)^2 \left[ 1 + \sum_{k=-\infty}^{\infty} \theta_k e^{iku} \right]$$

Assume the solution of Hill's equation has the form

$$\eta = \sum_{k=-\infty}^{\infty} \eta_k e^{i(k+c)u}$$

Substitution of the expressions for  $\Theta(u)$  and  $\eta$  into Hill's equation produces a set of identities from which successive approximations for  $c$  can be made.

From the assumed form of the solution, notice that if  $c$  is real, stability exists since  $\eta$  must be periodic and the transversal displacement is bounded. However, for  $c$  complex, the orbit is unstable since  $\eta$  then increases without bound either when time increases or decreases to infinity.

The orbits appear unstable since three approximations to  $c$  all prove complex. In all cases, the second and third estimations for  $c$  agree to two significant figures indicating probably convergence of the sequence. This indicated instability for the first order study, especially for the orbits of small values of  $\lambda$ , leads to contradictory conclusions. For infinitesimal orbits, the actual motion of a non-periodic Trojan will never deviate substantially from the equilateral libration point. Therefore, at least for small orbits, the motion should be stable. It appears that for the short period orbits the oscillation of  $\eta$  does not remain infinitesimally small, and large values of  $\eta$  destroy the first order accuracy. A higher order study should clarify this stability problem.

## 8. CONCLUSION

Several members of this family of short period Trojan orbits closely resemble those found by Willard except for larger values of  $\lambda$ ; however, he himself

questions the results for his large orbits. In this present work, sixteen significant digits were carried throughout the computations and a minimum of twelve figures of accuracy were obtained. The Jacobi constant, computed at each step of the integration agrees to at least eleven significant places.

As  $\lambda$  decreases from the branch point for Type II orbits, the general trend of the family is well indicated. The orbits pass closer and closer to the Sun while bending further around it. Still, it is difficult to visualize a natural ending to the family. Collision with the Sun is the most probable. This question is left for further study.

#### ACKNOWLEDGMENTS

The author wishes to thank Dr. Eugene Rabe of the University of Cincinnati for his guidance throughout the progress of this work.

#### REFERENCES

- Charlier, C. V. L., 1905, *Mechanik des Himmels*, (Verlag Von Veit and Comp).
- Message, P. J., 1959, *Astron. J.*, 64, 226.
- Rabe, E., 1961, *Astron. J.*, 66, 500.
- Steffensen, J. F., 1956, *Kgl Danske Videnskab. Selskab, Mat.-fys. Medd.* 30, No. 18.
- Willard, H. R., 1913, *Monthly Notices of R. A. S.*, 73, 471.



Table I

## Initial Conditions for Type I Short Period Orbits

$\lambda$	$x_0$	$y_0$	$\dot{x}_0$	$\dot{y}_0$
.02	.490 000 000	.883 345 912	.034 212 992	.020 214 565
.04	.480 000 000	.900 666 420	.067 699 676	.049 035 041
.06	.470 000 000	.917 986 928	.100 497 749	.062 143 545
.08	.460 000 000	.935 307 446	.132 643 610	.083 838 047
.10	.450 000 000	.952 627 944	.164 172 472	.106 002 435
.12	.440 000 000	.969 948 452	.195 118 459	.128 636 650
.14	.430 000 000	.987 268 960	.225 514 747	.151 741 902
.16	.420 000 000	1.004 589 478	.255 393 641	.175 323 990
.18	.410 000 000	1.021 909 986	.284 786 831	.199 393 764
.20	.400 000 000	1.039 230 485	.313 725 469	.223 967 746
.22	.390 000 000	1.056 550 993	.342 240 428	.249 063 981
.24	.380 000 000	1.073 871 501	.370 362 551	.274 728 209
.26	.370 000 000	1.091 192 009	.398 122 977	.300 985 453
.28	.360 000 000	1.108 512 527	.425 553 556	.327 892 236
.30	.350 000 000	1.125 833 025	.452 687 410	.355 514 710
.32	.340 000 000	1.143 153 533	.479 559 700	.383 938 172
.34	.330 000 000	1.160 474 041	.506 208 733	.413 273 799
.36	.320 000 000	1.177 794 549	.532 677 605	.443 668 953
.38	.310 000 000	1.195 115 057	.559 016 792	.475 323 993
.40	.300 000 000	1.212 435 565	.585 288 470	.508 520 700
.42	.290 000 000	1.229 756 073	.611 574 310	.543 674 791
.44	.280 000 000	1.247 076 581	.637 991 023	.581 442 614
.46	.270 000 000	1.264 397 090	.664 726 267	.622 971 901
.48	.260 000 000	1.281 717 600	.692 142 897	.670 643 365
.50	.250 000 000	1.299 038 106	.721 255 887	.731 531 835

Table II

Values of  $\mu$ ,  $\nu$ , T, C for Type I Orbits

	$\mu$	$\nu$	T	C
.02	.590 844 686	.039 738 614	6.300 603 307	3.002 469 808
.04	.604 656 383	.079 113 360	6.300 560 685	3.001 283 555
.06	.618 387 438	.118 160 867	6.300 489 448	2.999 297 572
.08	.632 054 922	.156 917 640	6.300 389 288	2.996 498 052
.10	.645 677 281	.195 420 360	6.300 259 756	2.992 865 000
.12	.659 274 632	.233 706 228	6.300 100 256	2.988 371 681
.14	.672 869 115	.271 813 357	6.299 910 032	2.982 983 933
.16	.686 485 339	.309 781 235	6.299 688 156	2.976 659 259
.18	.700 150 929	.347 651 280	6.299 433 511	2.969 345 680
.20	.713 897 237	.385 467 535	6.299 144 770	2.960 980 227
.22	.727 760 256	.423 277 530	6.298 820 369	2.951 486 985
.24	.741 781 825	.461 133 395	6.298 458 466	2.940 774 502
.26	.756 011 259	.499 093 326	6.298 056 899	2.928 732 318
.28	.770 507 569	.537 223 555	6.297 613 110	2.915 226 242
.30	.785 342 605	.575 601 077	6.297 124 059	2.900 091 769
.32	.800 605 580	.614 317 529	6.296 586 078	2.883 124 701
.34	.816 409 835	.653 484 894	6.295 994 677	2.864 067 354
.36	.832 903 333	.693 244 236	6.295 344 227	2.842 587 507
.38	.850 285 716	.733 779 716	6.294 627 459	2.818 244 797
.40	.868 837 720	.775 342 438	6.293 834 611	2.790 433 880
.42	.888 975 849	.818 294 210	6.292 951 849	2.758 280 861
.44	.911 364 883	.863 196 419	6.291 958 085	2.720 434 612
.46	.937 185 623	.911 018 660	6.290 817 485	2.674 581 000
.48	.968 937 726	.963 755 318	6.289 457 405	2.616 020 220
.50	1.014 247 299	1.027 301 748	6.287 665 797	2.531 098 829

Table III

## Initial Conditions for Type II Short Period Orbits

$\lambda$	$x_0$	$y_0$	$\dot{x}_0$	$\dot{y}_0$
.51	.245 000 000	1.307 698 360	.750 773 138	.875 606 527
.50	.250 000 000	1.299 038 106	.744 193 944	.909 782 831
.49	.255 000 000	1.290 377 852	.735 677 484	.930 854 592
.48	.260 000 000	1.281 717 598	.726 306 297	.946 762 135
.47	.265 000 000	1.273 057 344	.716 385 031	.959 686 855
.46	.270 000 000	1.264 397 090	.706 053 775	.970 609 262
.45	.275 000 000	1.255 736 835	.695 391 653	.980 070 591
.44	.280 000 000	1.247 076 581	.684 449 000	.988 407 217
.43	.285 000 000	1.238 416 327	.673 260 456	.995 845 229
.42	.290 000 000	1.229 756 073	.661 851 234	1.002 545 323
.41	.295 000 000	1.221 095 819	.650 240 472	1.008 626 625
.40	.300 000 000	1.212 435 565	.638 443 171	1.014 180 390
.39	.305 000 000	1.203 775 311	.626 471 402	1.019 278 400
.38	.310 000 000	1.195 115 057	.614 335 072	1.023 978 354
.37	.315 000 000	1.186 454 803	.602 042 457	1.028 327 485
.36	.320 000 000	1.177 794 549	.589 600 559	1.032 365 065

Table IV

Values of  $\rho$ ,  $\nu$ , T, C for Type II Orbits

$\lambda$	$\rho$	$\nu$	T	C
.51	1.166 273 116	1.153 406 735	6.283 419 569	2.277 381 564
.50	1.222 507 706	1.175 384 799	6.282 467 090	2.204 918 285
.49	1.265 302 544	1.186 470 240	6.281 900 834	2.157 773 902
.48	1.303 530 121	1.193 264 169	6.281 486 197	2.120 965 157
.47	1.339 624 384	1.197 583 555	6.281 158 537	2.090 320 805
.46	1.374 695 946	1.200 247 589	6.280 888 762	2.063 941 724
.45	1.409 379 285	1.201 710 412	6.280 660 813	2.040 765 689
.44	1.444 091 842	1.202 255 905	6.280 464 722	2.020 123 410
.43	1.479 138 155	1.202 076 271	6.280 293 806	2.001 558 590
.42	1.514 759 316	1.201 309 361	6.280 143 329	1.984 742 094
.41	1.551 159 407	1.200 058 473	6.280 009 797	1.969 426 214
.40	1.558 521 009	1.198 403 750	6.279 890 547	1.955 418 229
.39	1.627 015 052	1.196 409 158	6.279 783 497	1.942 564 151
.38	1.666 807 577	1.194 126 982	6.279 686 988	1.930 738 219
.37	1.708 064 726	1.191 600 830	6.279 599 668	1.919 835 830
.36	1.750 956 726	1.188 867 717	6.279 520 427	1.909 768 630

Table V

## Approximate Elliptical Elements for Type I Orbits

	a	e
.02	1.001 088 026	.018 895 816
.04 <sup>JO</sup>	1.001 215 557	.038 773 078
.06	1.001 338 042	.058 705 611
.08	1.001 455 229	.078 723 303
.10	1.001 566 852	.098 857 501
.12	1.001 672 630	.119 141 244
.14	1.001 772 255	.139 609 582
.16	1.001 865 389	.160 299 685
.18	1.001 951 656	.181 252 776
.20	1.002 030 633	.202 511 962
.22	1.002 101 842	.224 125 930
.24	1.002 164 741	.246 148 665
.26	1.002 218 706	.268 641 255
.28	1.002 263 019	.291 673 953
.30	1.002 296 844	.315 329 050
.32	1.002 319 195	.339 704 979
.34	1.002 328 893	.364 922 354
.36	1.002 324 502	.391 133 226
.38	1.002 304 221	.418 535 918
.40	1.002 265 708	.447 400 242
.42	1.002 205 770	.478 113 729
.44	1.002 119 722	.511 275 355
.46	1.001 999 921	.547 915 260
.48	1.001 831 487	.590 143 082
.50	1.001 572 690	.644 166 981

Table VI

Approximate Elliptical Elements for Type II Orbits

	a	e
.51	1.000 817 788	.769 986 921
.50	1.000 623 785	.798 637 191
.49	1.000 504 385	.815 877 208
.48	1.000 415 094	.828 623 875
.47	1.000 343 471	.838 781 100
.46	1.000 283 851	.847 205 780
.45	1.000 233 066	.854 371 430
.44	1.000 189 133	.860 572 473
.43	1.000 150 706	.866 003 795
.42	1.000 116 821	.870 814 967
.41	1.000 086 763	.875 101 074
.40	1.000 059 980	.878 944 708
.39	1.000 036 038	.882 408 323
.38	1.000 014 588	.885 541 970
.37	.999 995 343	.888 386 466
.36	.999 978 066	.890 975 601

Figure	Caption
1	The rotating coordinate system with a typical periodic orbit.
2	Short period orbits for $\epsilon = .12, .24, .36, .48$ .
3	Short period orbit for $\epsilon = .50$ and the branch point orbit.
4	Type II short period orbits for $\epsilon = .48, .42, .36$ .
5	Type I and Type II short period orbits for $\epsilon = .10$ .
6	Variation of $\epsilon$ with $\delta$ for periodic orbits.
7	Variation of $\delta$ with $\epsilon$ for periodic orbits.
8	Short and long period orbits for $\epsilon = .02$ .